ADVANCED MATERIALS

Supporting Information

for *Adv. Mater.*, DOI 10.1002/adma.202507893

Bimetallic Nanocluster-Based Light-Emitting Diodes With High External Quantum Efficiency and Saturated Red Emission

Jose V. Rival, Savita Chand, Arijit Jana, Nonappa, Vasudevanpillai Biju, Thalappil Pradeep, Pachaiyappan Rajamalli and Edakkattuparambil Sidharth Shibu**

Supporting Information

Bimetallic Nanocluster-based Light-Emitting Diodes with High External Quantum Efficiency and Saturated Red Emission

Jose V. Rival,[a] Savita Chand,[b] Arijit Jana,[c] Nonappa,[d] Vasudevanpillai Biju,[e] Thalappil Pradeep,[c] Pachaiyappan Rajamalli,[b] Edakkattuparambil Sidharth Shibu[a]**

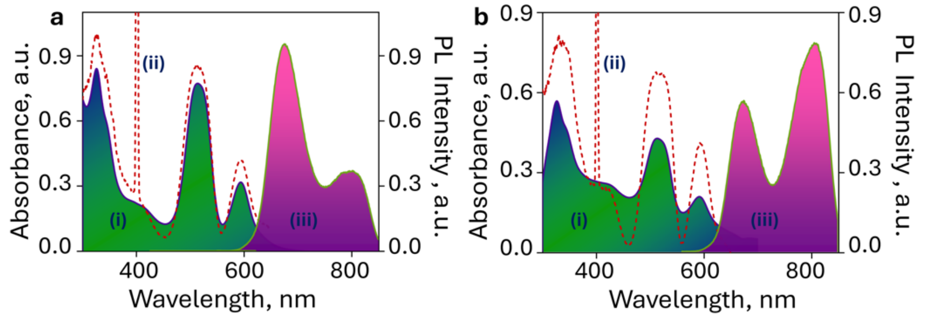

Figure S1. (i) UV/Vis absorption, (ii) excitation (corresponding to the emissions at 798 and 806 nm from $[Au_2Cu_6(Sadm)_6(DPPEO)_2]$ and $[Au_2Cu_6(Sadm)_6(TPP)_2]$ NCs, respectively) and PL (iii) spectra of (a) $[Au_2Cu_6(Sadm)_6(DPPEO)_2]$ and (b) $[Au_2Cu_6(Sadm)_6(TPP)_2]$ NCs.

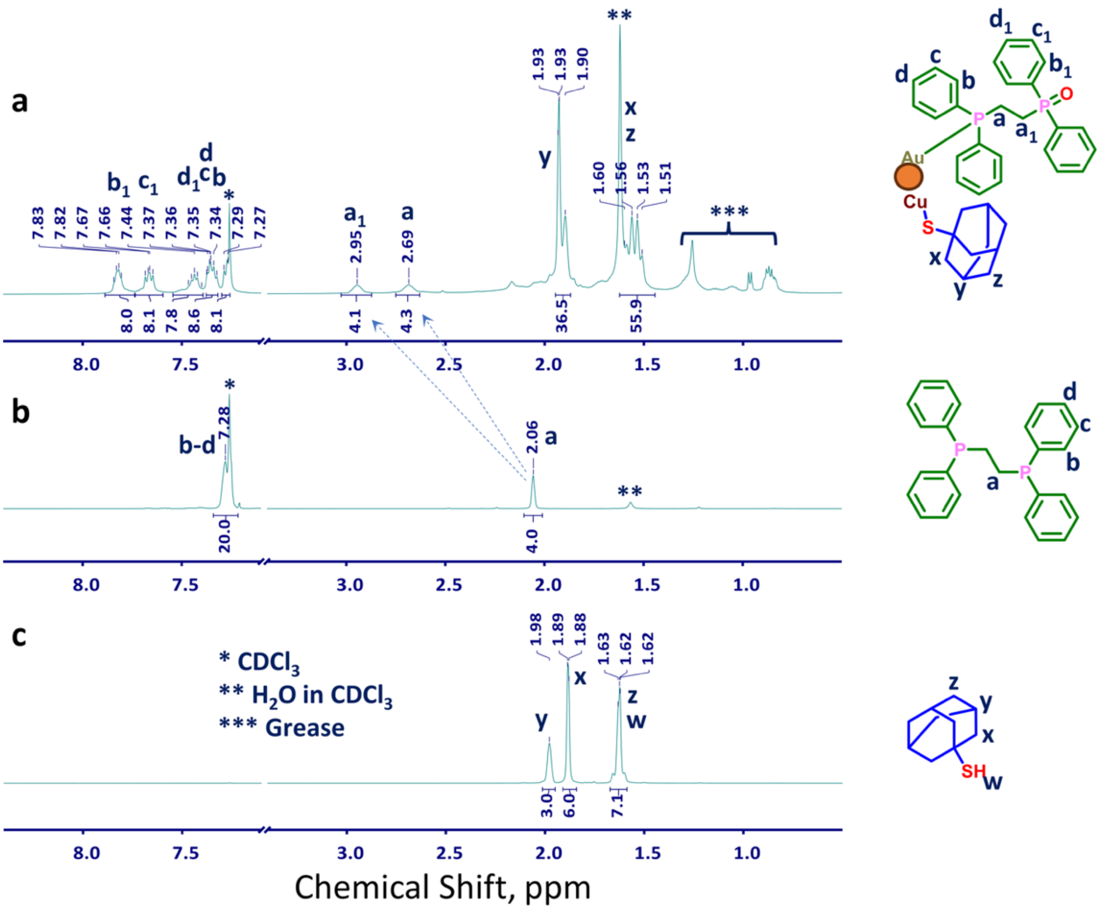

Figure S2. ^{1}H NMR spectra of (a) $[Au_2Cu_6(Sadm)_6(DPPEO)_2]$ NC, (b) DPPE, and (c) HSadm.

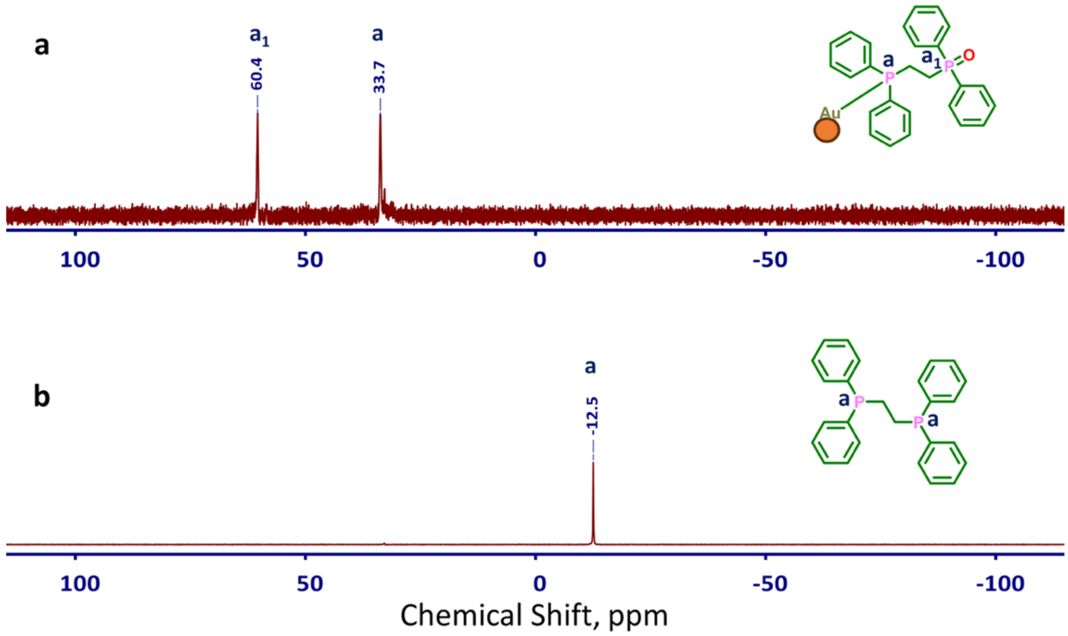

Figure S3. ^{31}P NMR spectra of (a) [$Au_2Cu_6(Sadm)_6(DPPEO)_2$] NC and (b) DPPE ligand in $CDCl_3$.

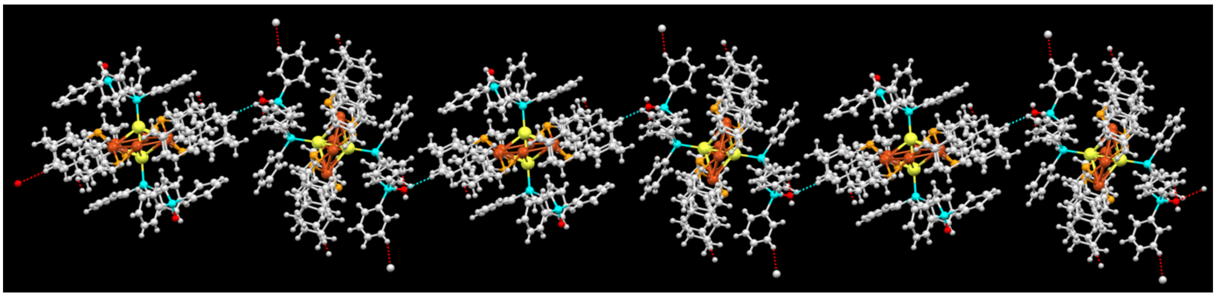

Figure S4. The C–H···O interactions between the neighboring NCs in the crystal resulted in a zig-zag tape arrangement of NCs.

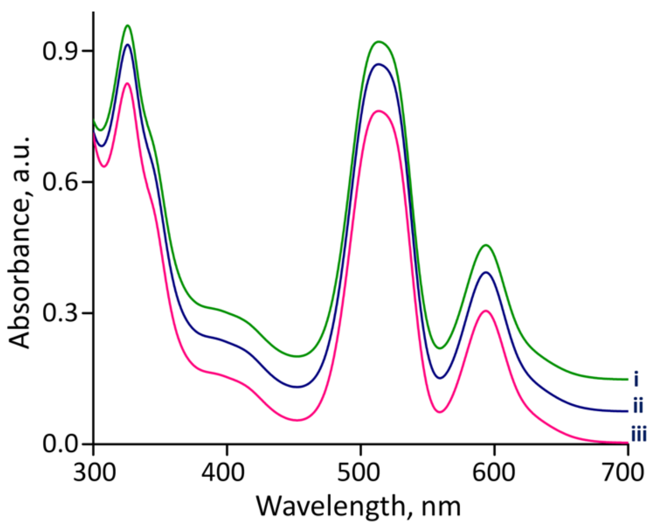

Figure S5. UV/Vis absorption spectra of NC solution recorded under (i) argon, (ii) ambient, and (iii) oxygen atmospheres (for clarity, spectra were vertically translated).

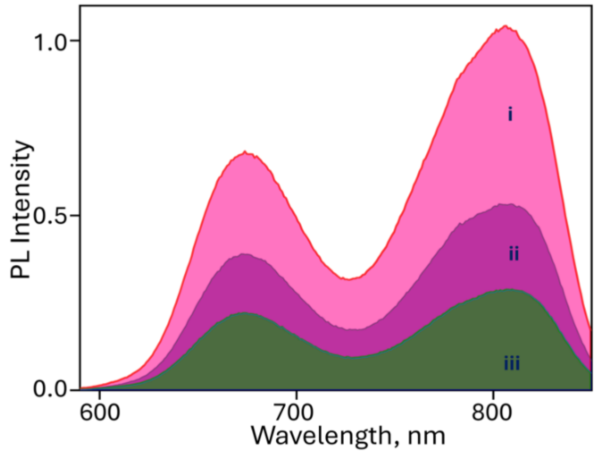

Figure S6. PL spectra of $[Au_2Cu_6(Sadm)_6(TPP)_2]$ NC solution NC solution recorded under (i) argon, (ii) ambient, and (iii) oxygen atmospheres.

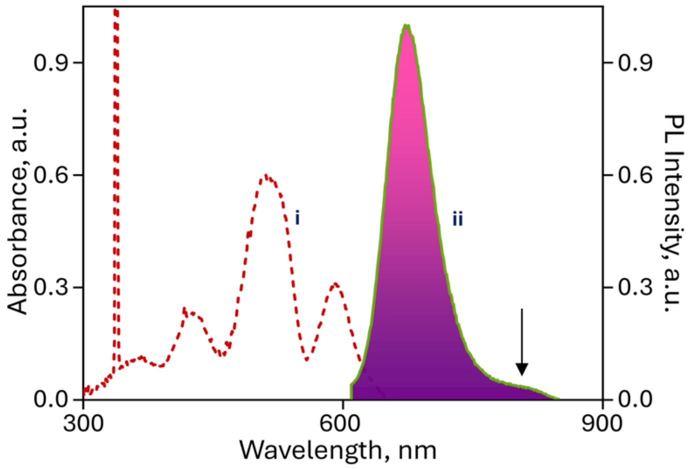

Figure S7. Excitation (i) and emission (ii) spectra of $[Au_2Cu_6(Sadm)_6(TPP)_2]$ NC.

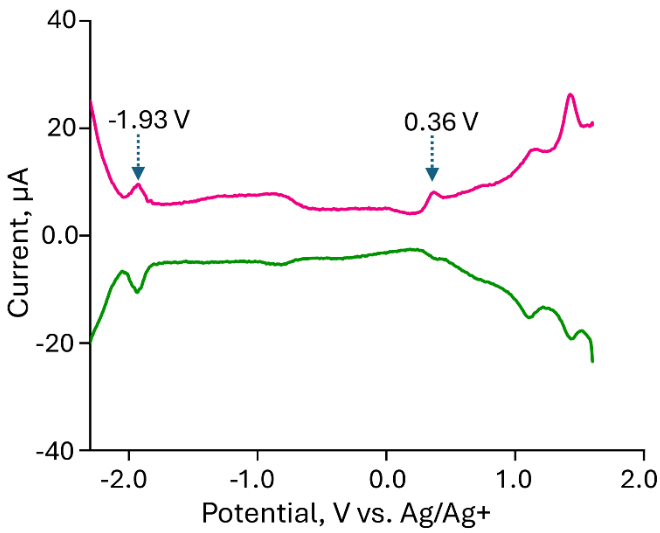

Figure S8. Differential pulse voltammetry (DPV) of $[Au_2Cu_6(Sadm)_6(DPPEO)_2]$ (20 μM) in acetonitrile/toluene mixture (1:1).

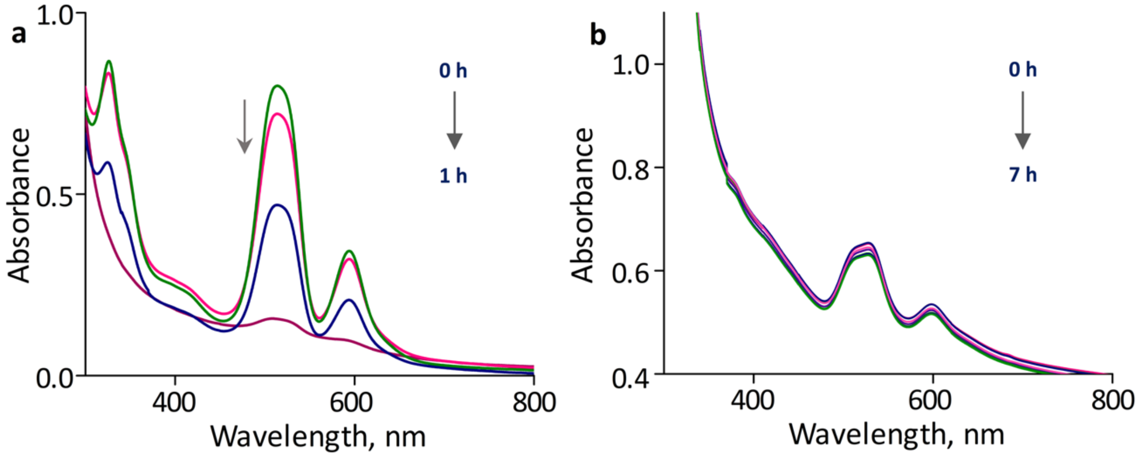

Figure S9. Temporal UV/Vis absorption spectra recorded from (a) NC solution and (b) NC film under UV illumination.

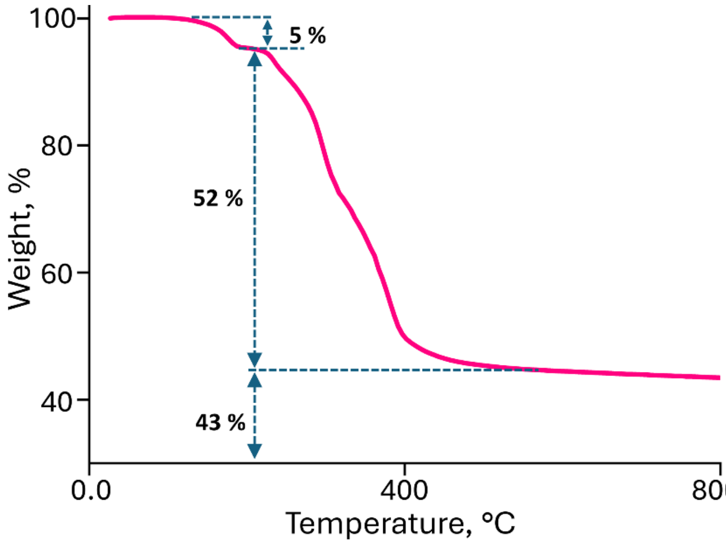

Figure S10. TGA curve of $[Au_2Cu_6(Sadm)_6(DPPEO)_2]$ NC.

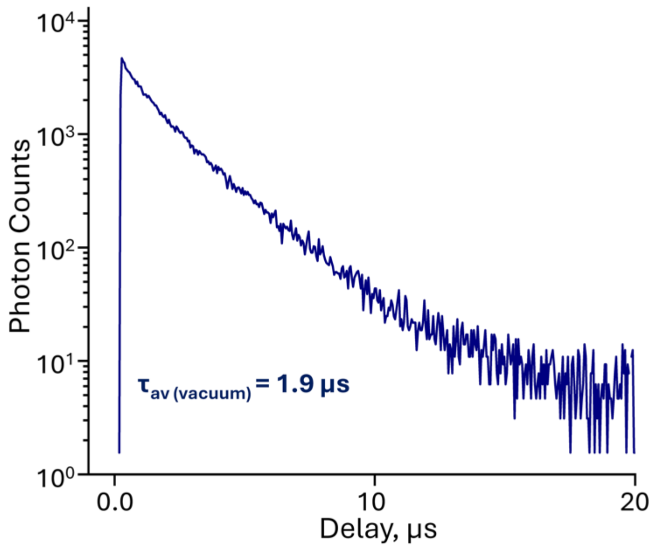

Figure S11. The PL decay profile of NC solid under vacuum.

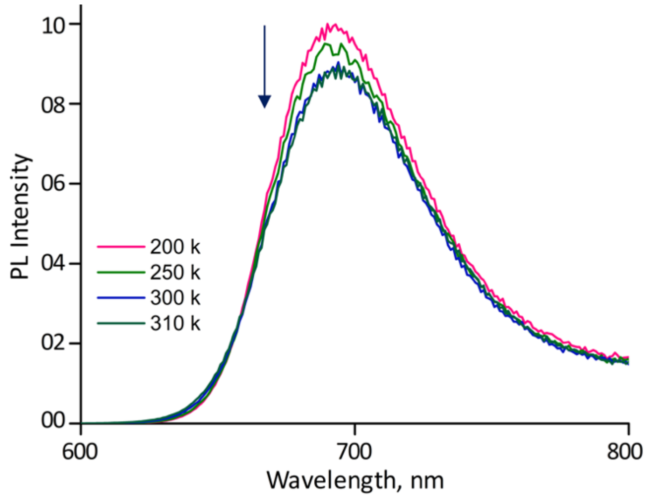

Figure S12. The temperature-dependent PL spectra recorded from NC solid.

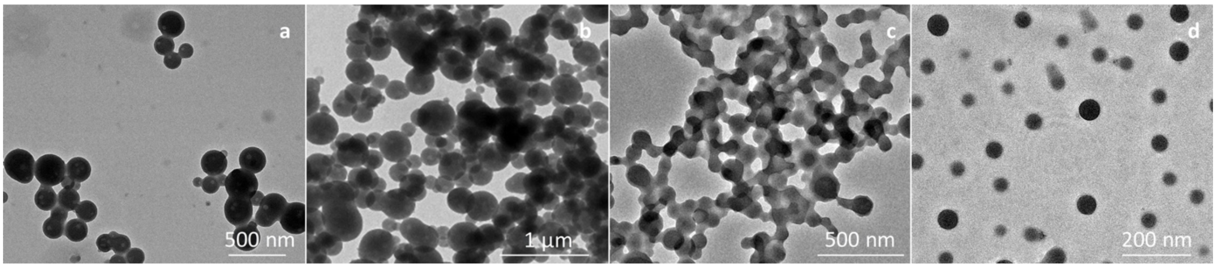

Figure S13. TEM micrographs of assembled-NCs at (a) 50%, (b) 60%, (c) 70%, and (d) 90% f_w.

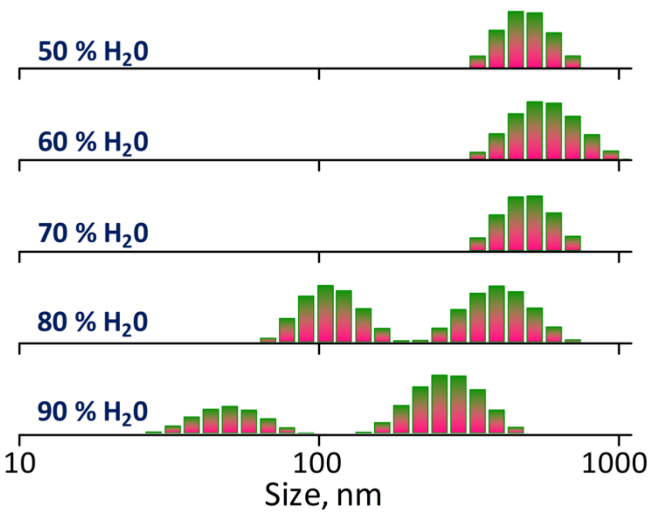

Figure S14. DLS spectra of [$Au_2Cu_6(Sadm)_6(DPPEO)_2$] NCs in THF at different f_w.

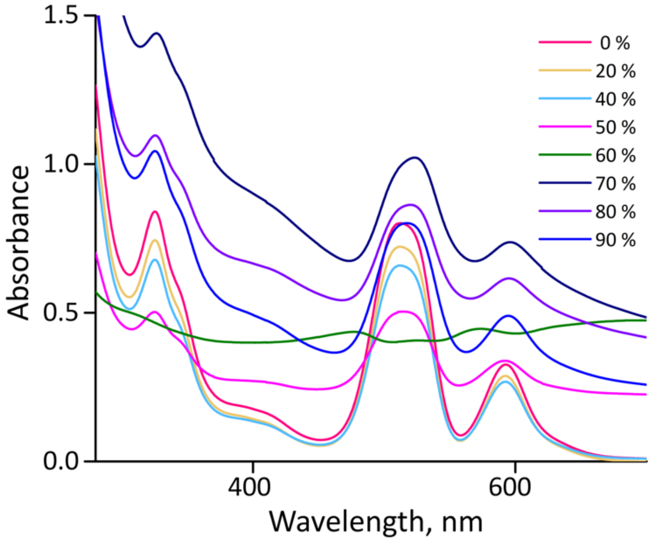

Figure S15. The UV/Vis absorption spectra of NC solution at different f_w.

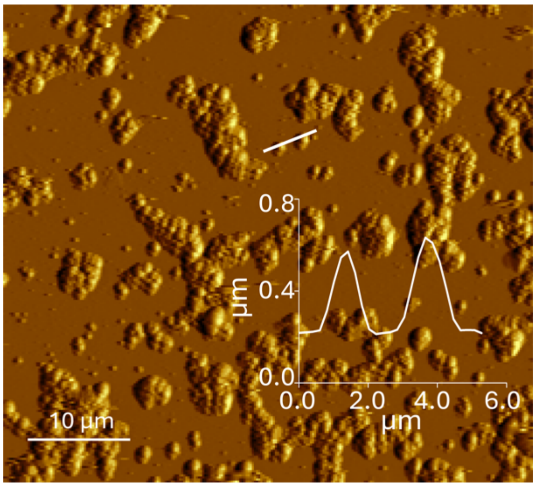

Figure S16. A large area AFM image of assembled-NCs (60% f_w). The height profile is shown in the inset.

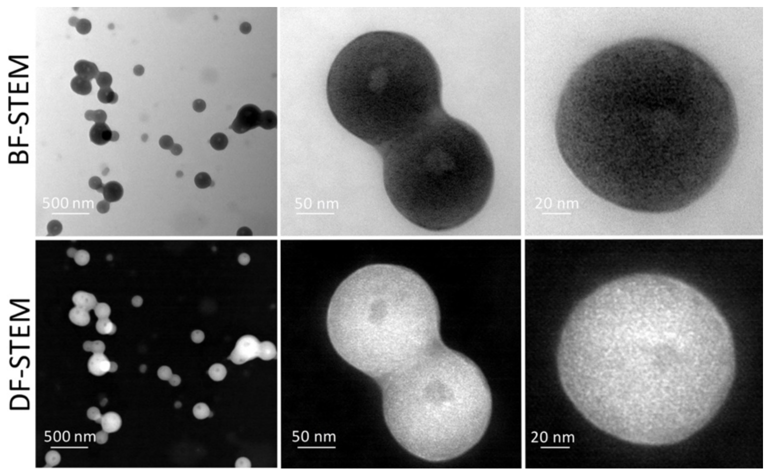

Figure S17. BF- and DF-STEM images show large area assembly, and assembled dimer and monomer.

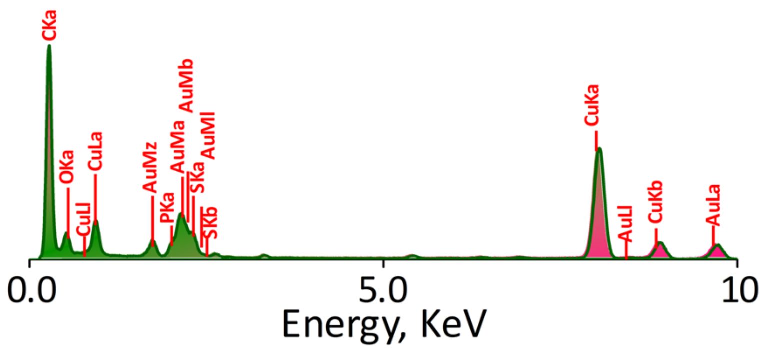

Figure S18. The EDS spectrum of assembled superstructures (f_w = 60%). Respective elements are labeled.

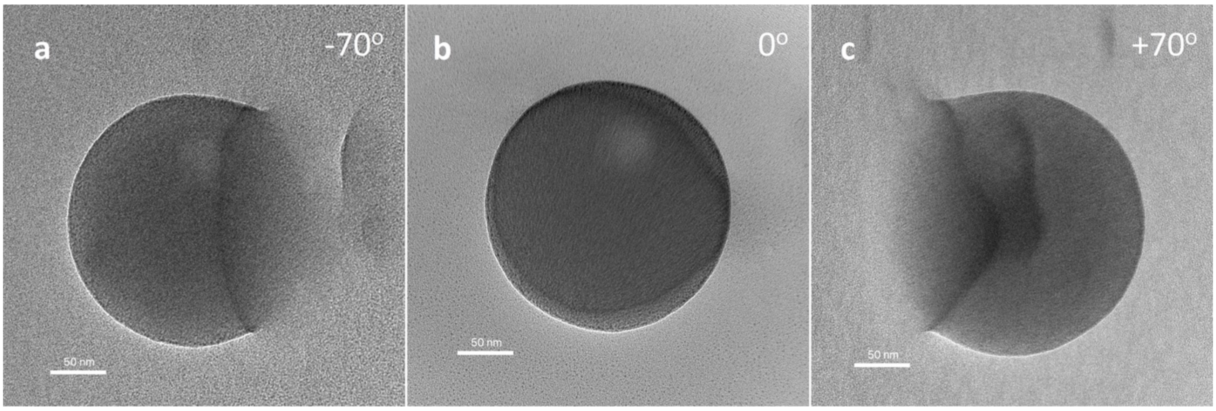

Figure S19. BF-TEM micrographs of [$Au_2Cu_6(Sadm)_6(DPPEO)_2$] NC assembly ($f_w$ = 60%) at different tilt angles.

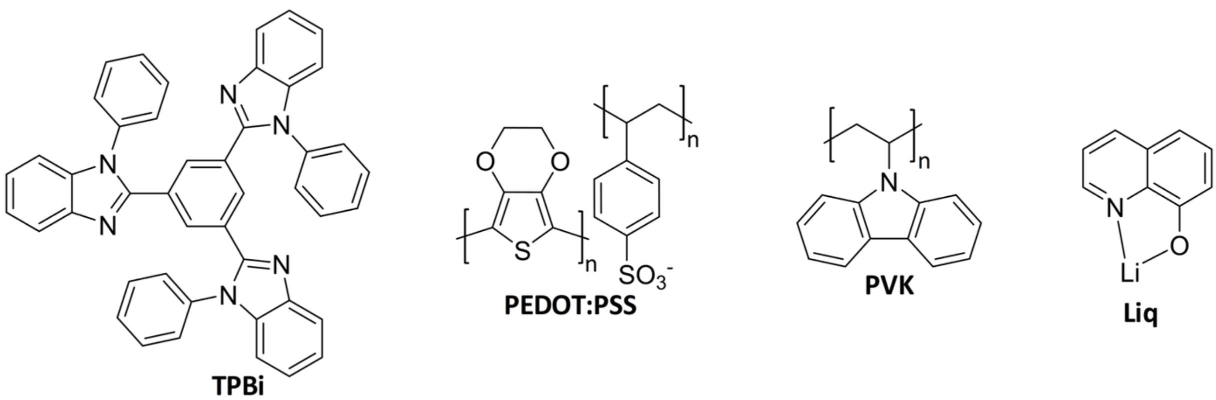

Figure S20. The chemical structure of different organic materials used for LED fabrication.

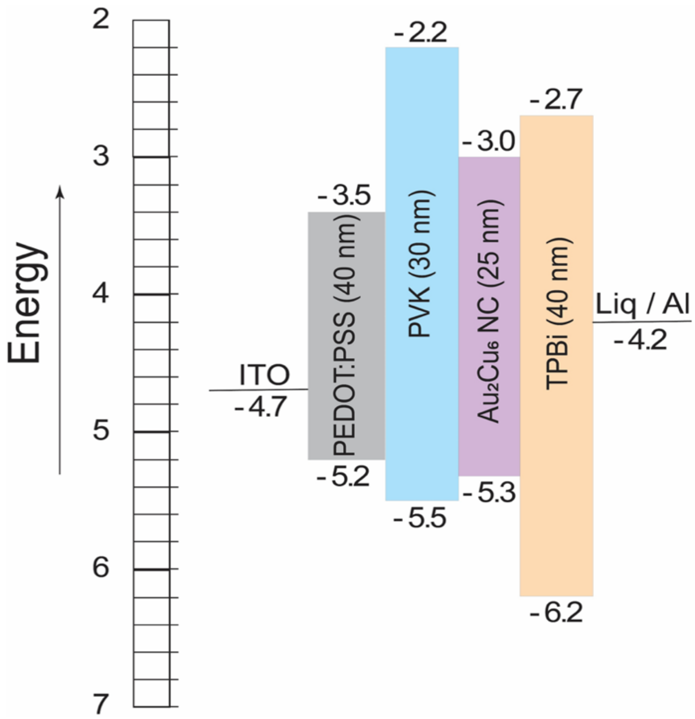

Figure S21. The energy level alignment in the device.

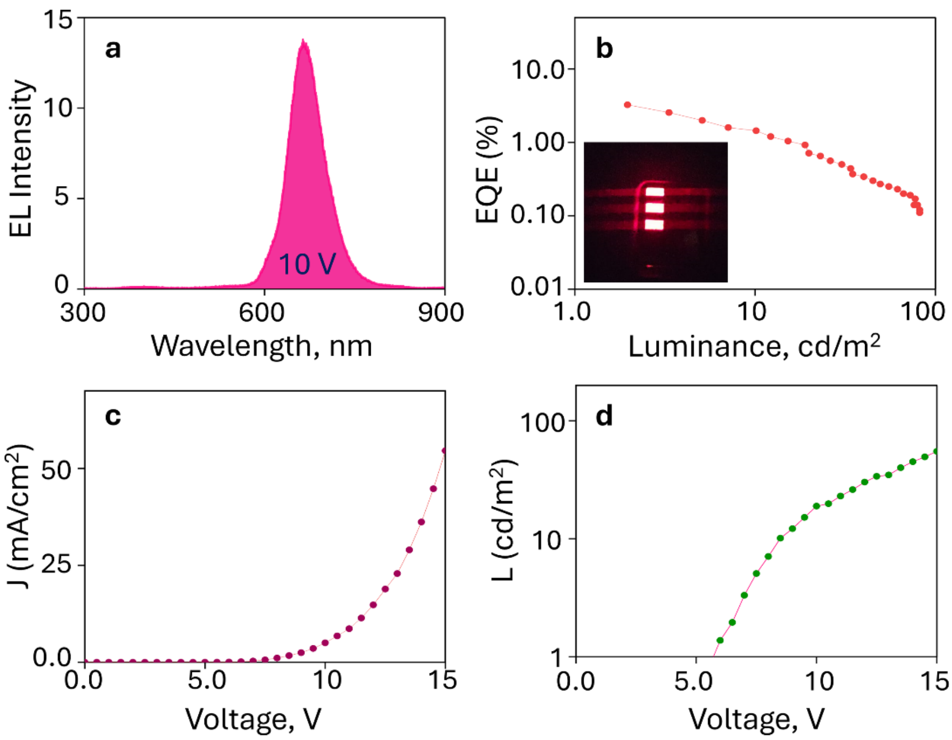

Figure S22. (a) EL spectra of [$Au_2Cu_6(Sadm)_6(TPP)_2$] NC-based device at 10V. (b) EQE *vs* luminance curve. The inset shows a photograph of the fabricated LED device. (c) Current density-voltage curve of the device. (d) Luminance-voltage curve of the device.

Light emitting NC Layer	PLQY (%)	L_{max} (cd m^{-2})	Wavelength (nm)	EQE_{max} (%)	CIE Coordinates (x, y)	Ref.
Au_{25} or Ag_{25}	_	_	750	0.013	_	1
Au@GSH	15	40	625	0.12	(0.57– 0.59, 0.40 – 0.41)	2
Au@TOP	4.99	100	White light	0.08	(0.27,0.33)	3
$(Au_4L_4)_n/(Au_4D_4)_n$	41.4	_	503	1.5	_	4
TOAB/Arg/ATT@Au	73.4	1104	544	5.1	(0.31,0.65)	5
Au_4Ag_2	77.2	8804	539	7.0 (d)	_	6
Ag_6Cu	78	184	573	13.9 (d)	_	7
$PtAu_3$	90	1000	588	18.1 (d)	(0.33,0.61)	8
$PtAu_3$	90.1	6539	556	16.6 (d)	(0.30,0.61)	9
Au_3Ag	25	5211	440	2.06 (d)	(0.16,0.09)	10
Ag_8Au_{10}	77	14,859	567	15.7 (d)	(0.4714,0.5200)	11
Ag_3Cu_5	75	8554	585	14.7 (d)	(0.51,0.48)	12
R/S-Cu_2Au_2	94/ 89	2010/1670	564	36.5% (d) 23.5/20.8 (nd)	(0.395,0.572) (0.394,0.574)	13
$[Au_2Cu_6(Sadm)_6(DPPEO)_2]$	**62**	**1246**	**668**	**12.6 (nd)**	**(0.70,0.30)**	**Current Work**
$[Au_2Cu_6(Sadm)_6(TPP)_2]$	**17.8**	**55.17**	**666**	**3.24 (nd)**	**(0.67,0.31)**	**Current Work**
$[DBFDP]_2Cu_4I_4$	5	1500	White light	0.73 (d)	(0.37,0.45)	14
$[DtBCzDBFDP]_2Cu_4I_4$	65	7000	491	7.9 (d)	(0.22,0.43)	15
$[DPACDBFDP]_2Cu_4I_4$	81	4000	500	19.5 (d)	(0.21±0.1,0.45 ± 0.1)	16
$[TMeOPP]_4Cu_4I_4$	99	10710	550	15.6 (d)	(0.40±0.05, 0.53±0.04)	17
$Cu_2I_2[P\text{-}m\text{-}(Tol)_3]_2$Pyrphos	90	1426	560	19.1 (d)		18
$Cu_6I_6(ppda)_2$	36	_	564	0.31 (d)	(0.43,0.51)	19
$Cu_2I_2(BINAP)_2$	4.7	1200	515	0.54	_	20
$[DDMACDBFDP]_2Cu_4I_4$	99	5502	504	29.4 (d) 9.5 (nd)	(0.21,0.50)	21

Table S1. The comparison table shows the details of reported NCs in the device fabrication (d- doped and nd- non-doped).

References

[1] B. Niesen, B. P. Rand, *Adv. Mater.* **2014**, *26*, 1446.

[2] T.-W. Koh, A. M. Hiszpanski, M. Sezen, A. Naim, T. Galfsky, A. Trivedi, Y.-L. Loo, V. Menon, B. P. Rand, *Nanoscale* **2015**, *7*, 9140.

[3] Y.-C. Chao, K.-P. Cheng, C.-Y. Lin, Y.-L. Chang, Y.-Y. Ko, T.-Y. Hou, C.-Y. Huang, W. H. Chang, C.-A. J. Lin, *Sci. Rep.* **2018**, *8*, 8860.

[4] Z. Han, X. Zhao, P. Peng, S. Li, C. Zhang, M. Cao, K. Li, Z.-Y. Wang, S.-Q. Zang, *Nano Res.* **2020**, *13*, 3248.

[5] Y. Tian, W. Zheng, X. Zhang, Y. Wang, Y. Xiao, D. Yao, H. Zhang, *Nano Lett.* **2023**, *23*, 4423.

[6] L. Xu, J. Wang, X. Zhu, X. Zeng, Z. Chen, *Adv. Funct. Mater.* **2015**, *25*, 3033.

[7] L.-J. Xu, X. Zhang, J.-Y. Wang, Z.-N. Chen, *J. Mater. Chem. C* **2016**, *4*, 1787.

[8] N. Natarajan, L.-X. Shi, H. Xiao, J.-Y. Wang, L.-Y. Zhang, X. Zhang, Z.-N. Chen, *J. Mater. Chem. C* **2018**, *6*, 8966.

[9] N. Natarajan, L.-X. Shi, H. Xiao, J.-Y. Wang, L.-Y. Zhang, X. Zhang, Z.-N. Chen, *J. Mater. Chem. C* **2019**, *7*, 2604.

[10] J. Ni, C. Zhong, L. Li, M. Su, X. Wang, J. Sun, S. Chen, C. Duan, C. Han, H. Xu, *Angew. Chem. Int. Ed.* **2022**, *61*, e202213826.

[11] Y.-Z. Huang, L.-X. Shi, J.-Y. Wang, H.-F. Su, Z.-N. Chen, *ACS Appl. Mater. Interfaces* **2020**, *12*, 57264.

[12] Z. Jiao, M. Yang, J.-Y. Wang, Y.-Z. Huang, P. Xie, Z.-N. Chen, *J. Mater. Chem. C* **2021**, *9*, 5528.

[13] J. Lu, B. Shao, R.-W. Huang, L. Gutiérrez-Arzaluz, S. Chen, Z. Han, J. Yin, H. Zhu, S. Dayneko, M. N. Hedhili, X. Song, P. Yuan, C. Dong, R. Zhou, M. I. Saidaminov, S.-Q. Zang, O. F. Mohammed, O. M. Bakr, *J. Am. Chem. Soc.* **2024**, *146*, 4144.

[14] M. Xie, C. Han, J. Zhang, G. Xie, H. Xu, *Chem. Mater.* **2017**, *29*, 6606.

[15] M. Xie, C. Han, Q. Liang, J. Zhang, G. Xie, H. Xu, *Sci. Adv.* **2019**, *5*, eaav9857.

[16] N. Zhang, H. Hu, L. Qu, R. Huo, J. Zhang, C. Duan, Y. Meng, C. Han, H. Xu, *J. Am. Chem. Soc.* **2022**, *144*, 6551.

[17] Y. Li, S. Xu, X. Zhang, Y. Man, J. Zhang, G. Zhang, S. Chen, C. Duan, C. Han, H. Xu, *Angew. Chem. Int. Ed.* **2023**, 62, e202308410.

[18] J.-J. Wang, L.-Z. Feng, G. Shi, J.-N. Yang, Y.-D. Zhang, H. Xu, K.-H. Song, T. Chen, G. Zhang, X.-S. Zheng, F. Fan, Z. Xiao, H.-B. Yao, *Nat. Photon.* **2024**, *18*, 200.

[19] K. Xu, B.-L. Chen, R. Zhang, L. Liu, X.-X. Zhong, L. Wang, F.-Y. Li, G.-H. Li, K. A. Alamry, F.-B. Li, W.-Y. Wong, H.-M. Qin, *Dalton Trans.* **2020**, *49*, 5859.

[20] J.-J. Wang, H.-T. Zhou, J.-N. Yang, L.-Z. Feng, J.-S. Yao, K.-H. Song, M.-M. Zhou, S. Jin, G. Zhang, H.-B. Yao, *J. Am. Chem. Soc.* **2021**, *143*, 10860.

[21] N. Zhang, Y. Li, S. Han, Y. Wei, H. Hu, R. Huo, C. Duan, J. Zhang, C. Han, G. Xie, H. Xu, *Angew. Chem. Int. Ed.* **2023**, *62*, e202305018.